The Planetary Science Journal, 2:195 (17pp), 2021 October https://doi.org/10.3847/PSJ/ac19b7

Tiger: Concept Study for a New Frontiers Enceladus Habitability Mission

Elizabeth M. Spiers[1], Jessica M. Weber[2], Chandrakanth Venigalla[3], Andrew M. Annex[4], Christine P. Chen[2], Carina Lee[5], Patrick Clifton Gray[6], Kathleen J. McIntyre[7], Jodi R. Berdis[8], Shane R. Carberry Mogan[9], Paula do Vale Pereira[10], Saroj Kumar[11], William O'Neill[12], Elizabeth A. Czajka[13], Perianne E. Johnson[14], Alyssa Pascuzzo[15], Sindhoora Tallapragada[16], Deanna Phillips[17], Karl Mitchell[2], Alfred Nash[2], Jennifer Scully[2], and Leslie Lowes[2]

[1] Department of Earth & Atmospheric Sciences, Georgia Institute of Technology, Atlanta, GA 30318, USA; spiers@gatech.edu
[2] NASA Jet Propulsion Laboratory, California Institute of Technology, Pasadena, CA 91109, USA
[3] Department of Aerospace Engineering Sciences, University of Colorado Boulder, Boulder, CO 80309, USA
[4] Department of Earth and Planetary Sciences, Johns Hopkins University, Baltimore, MD 21218, USA
[5] Lunar and Planetary Institute, Universities Space Research Association, Houston, TX 77058, USA
[6] Duke University Marine Laboratory, Nicholas School of the Environment, 135 Duke Marine Lab Road, Beaufort, NC 28516, USA
[7] Department of Physics, University of Central Florida, Orlando, FL 32618, USA
[8] Astronomy Department, New Mexico State University, Las Cruces, NM 88003, USA
[9] Center for Space Science, New York University Abu Dhabi, Abu Dhabi, UAE
[10] Department of Aeronautics and Astronautics, Massachusetts Institute of Technology, Cambridge, MA 02139, USA
[11] Propulsion Research Center, University of Alabama in Huntsville, Huntsville, AL 35899, USA
[12] Department of Aeronautical and Astronautical Engineering, Purdue University, West Lafayette, IN 47907, USA
[13] Department of Physics and Astronomy, University of Texas at San Antonio, San Antonio, TX 78249, USA
[14] Department of Astrophysical and Planetary Sciences, University of Colorado Boulder, Boulder, CO 80303, USA
[15] Department of Earth, Environmental, and Planetary Sciences, Brown University, Providence, RI 02912, USA
[16] Department of Astronautical Engineering, University of Southern California, Los Angeles, CA 90007, USA
[17] University of Alabama in Huntsville, Huntsville, AL 35899, USA
Received 2021 February 9; revised 2021 July 15; accepted 2021 July 19; published 2021 September 17

Abstract

Data returned from the Cassini–Huygens mission have strengthened Enceladus, a small icy moon of Saturn, as an important target in the search for life in our solar system. Information gathered from Cassini to support this includes the presence of a subsurface liquid water ocean, vapor plumes and ice grains emanating from its south polar region, and the detection of essential elements and organic material that could potentially support life. However, several outstanding questions remain regarding the connectivity of plume material to the ocean and the composition of the complex organic material. Herein we introduce Tiger, a mission concept developed during the 2020 Planetary Science Summer School at NASA's Jet Propulsion Laboratory. Tiger is a flyby mission that would help further constrain the habitability of Enceladus through two science objectives: (1) determine whether Enceladus's volatile inventory undergoes synthesis of complex organic species that are evidence for a habitable ocean, and (2) determine whether Enceladus's plume material is supplied directly from the ocean or if it interfaces with other reservoirs within the ice shell. To address the science goals in a total of eight flybys, Tiger would carry a four-instrument payload, including a mass spectrometer, a single-band ice-penetrating radar, an ultraviolet imaging spectrograph, and an imaging camera. We discuss Tiger's instrument and mission architecture, as well as the trades and challenges associated with a habitability-focused New Frontiers–class flyby mission to Enceladus.

Unified Astronomy Thesaurus concepts: Habitable planets (695); Saturnian satellites (1427); Ocean planets (1151); Astrobiology (74); Interdisciplinary astronomy (804)

1. Introduction

Enceladus, an icy Saturnian moon, has intrigued the planetary science community since its discovery in the late eighteenth century (Dougherty et al. 2018). While Enceladus was first imaged during Voyager 1 and Voyager 2 flybys, the Cassini–Huygens mission revealed the unique activity and characteristics of this fascinating satellite. The mission confirmed that Enceladus has a global, subsurface, liquid water ocean (Postberg et al. 2011; Thomas et al. 2016); active jets emanating from its southern polar region (Hansen et al. 2006; Porco et al. 2006; Spahn et al. 2006) containing complex organic material (Postberg et al. 2018b) that is believed to be formed from the ocean; and a geologically young surface, particularly in the southern hemisphere (Jaumann et al. 2007). The underlying ocean is believed to be salty (Postberg et al. 2009) and interact with a silicate interior that may have hydrothermal venting (Hsu et al. 2015; Waite et al. 2017). This ocean and any hydrothermal venting are likely to be maintained through tidal heating generated within the rocky core (Choblet et al. 2017).

Enceladus's ice shell undergoes daily tidal flexing, enhanced by the presence of a subsurface ocean (Nimmo et al. 2007). Energy generated through tidal flexing engenders large tidal stresses on the surface, resulting in the opening and closing of fractures, which are thought to travel through the entire depth of the ice shell (<5 km in the south polar region; Čadek et al. 2016), connecting to the underlying ocean, and are likely to be filled with liquid water (Spencer et al. 2018). The plume emanates from these "tiger stripe" fractures consisting primarily of two forms: wide, diffuse, curtain-like sprays (Spitale et al. 2015) and dense, narrow jets (Porco et al. 2014) and geysers (Goldstein et al. 2018). Particles embedded in the jets can escape Enceladus's gravity, supplying Saturn's E ring, and coat the surfaces of nearby satellites (Kempf et al. 2018). The curtains tend to reach relatively low altitudes (∼10 km) and thus likely consist of heavier materials that ultimately return to Enceladus's surface (Goldstein et al. 2018).

The plume is composed of vapor and particulates, the latter being primarily ice grains that vary in size, composition, and formation processes (Porco et al. 2006; Spahn et al. 2006; Schmidt et al. 2008; Postberg et al. 2009). Ice grains on the order of ∼1 μm likely originate either from salty-ocean spray or from vapor condensation within the subsurface fissures, while smaller nanometer-sized grains presumably condense from the vapor during expansion and cooling processes (Schmidt et al. 2008). A variety of organic and inorganic compounds have also been detected in the plume, as well as species indicative of hydrothermal activity and serpentinization (Waite et al. 2006, 2009; Postberg et al. 2008, 2009, 2018b, 2018a).

Owing to these combined discoveries, Enceladus has received significant attention for its astrobiological potential. The presence of organics and energy within an ocean world opens many possibilities for habitability and life detection investigations (McKay et al. 2018). It is considered one of the most promising targets for the search for life in our solar system, as mentioned in the 2013 Decadal Survey (National Academies of Sciences, Engineering, and Medicine 2018), the New Frontiers 4 (NF4) Announcement of Opportunity (AO; Niebur 2016), and the New Frontiers 5 (NF5) AO (Niebur 2020). In addition, the underlying liquid water within Enceladus can be directly examined by flying through its south polar plume. As Enceladus's plume is predictable and sourced from a liquid water ocean, it represents a unique opportunity to utilize a flyby mission architecture to directly sample materials from deep within a surface-frozen ocean world. In contrast, other ocean worlds like Europa likely require more complex, landed in situ mission designs to perform analysis of the interior, due to the irregular and spatiotemporal unconstrained nature of Europan plume activity (Rathbun & Spencer 2020). While missions such as Europa Clipper can assess the habitability of Europa through sampling of plume material if a plume is active during the mission duration, it is unknown whether the plume is directly sourced from the deeper interior (Howell & Pappalardo 2020). Therefore, an Enceladus flyby mission represents a unique and promising opportunity to examine the habitability of an ocean world.

Herein, we introduce the Tiger mission (mission logo shown in Figure 1), which was developed during the first session of the 2020 NASA Jet Propulsion Laboratory (JPL) Planetary Science Summer School (PSSS; Budney et al. 2018; Lowes et al. 2020). The NASA JPL PSSS is a rigorous 10-week program that conducts a prephase A concept study for a NF-class mission designed by graduate students and early career planetary scientists and engineers. The 2020 study culminated in a week-long, virtual session to formalize our proposed concept. The final week included trade study sessions with Team X (NASA JPL's advanced project design team) and a final presentation to a review panel.

Tiger is a habitability-focused, multi-flyby mission concept to Enceladus, concentrating on the south polar region. Tiger would build on the science achieved by Cassini in order to further constrain the environments within Enceladus and determine the habitability of the liquid water ocean and any connected reservoirs. In addition, Tiger would provide information necessary to guide future missions to ocean worlds with life detection/habitability-focused goals. A life detection mission to Enceladus would necessitate a flagship-class lander (e.g., Enceladus Orbilander, MacKenzie et al. 2020), which is not within the budgetary constraints of a NF-class mission. Tiger's mission objectives address key science questions in the 2013 Decadal Survey (National Academies of Sciences, Engineering, and Medicine 2018), as well as the "Roadmap to Ocean Worlds" (Hendrix et al. 2019). The Tiger mission concept and feasibility study showcases the science return of an NF-class mission to Enceladus and discusses the trades and challenges prescribed in adherence to NF requirements. In this work, we discuss both the proposed mission concept and these trades and challenges for the architecture of an NF-class habitability mission to Enceladus.

Figure 1. The logo for the Tiger mission, designed by PSSS participant Alyssa Pascuzzo.

2. Science

The Tiger mission focuses on better constraining the habitability of Enceladus through two specific scientific objectives (Figure 2). First, Tiger would assess the potential for habitability of the subsurface ocean by analyzing the organic material in the vapor and redox state of the ocean (Postberg et al. 2011). Second, Tiger would address the transport mechanisms for material from the subsurface ocean through the ice shell and into space as plume ejecta. These are expressed as the following science objectives:

Objective 1. Determine whether Enceladus's volatile inventory undergoes synthesis of complex organic species that are evidence for a habitable ocean.

Objective 2. Determine whether Enceladus's plume material is supplied directly from the ocean or if it interfaces with other reservoirs within the ice shell.

ASSESS THE HABITABILITY OF ENCELADUS'S OCEAN THROUGH UNDERSTANDING THE (1) ORGANIC MATTER AND (2) LIQUID WATER					
Science Objectives	Science Measurement Requirements		Instrument Requirements	Projected Performance[a]	Mission Requirements
	Physical Parameters	*Observables*			
1. Determine if Enceladus's volatile inventory undergoes synthesis of complex organic species that are evidence for a habitable ocean. *Enceladus's plume is known to be ejecting water vapor, ice grains, and organic materials, providing a unique opportunity to sample a potentially habitable environment. This objective seeks to utilize the plume to indirectly understand the organic and salt material of the ocean.* *To determine if synthesis is occurring, we would sample the plume to investigate if complex organic species are present or if the material is limited to simple products such as methane and benzene. We would also investigate whether sulfur is present in quantities compatible with habitability.*	**1.1 Determine whether key building blocks for life exist in Enceladus's ocean.** Definitive identification of organics present in the plume vapor. By identifying the materials present, we would better understand the reactions occurring within the plume/ocean. Specifically, we would look for reactive organic compounds including alcohols, amines, carboxylic acids as well as larger, more complex organics.	High resolution mass spectra (*m/z* ratios) of organic materials (expanding on Cassini; [1,2]).	**MS** *Range:* 1-500 amu *Resolution:* >10,000 m/Dm *Min. collector area:* 10x10 cm	**MASPEX** (MS) *Range:* 1-1000 amu *Resolution:* >30,000 m/Dm	MS pointing ram direction, UVS pointing nadir **MS**: Visual confirmation of active plumes through imaging. 7 flybys, triplicate at minimum, +1 contingency flyby. Velocity of vehicle between 4-6 km/s. **UVS**: SOs for the large SP plume; StOs for smaller jets, constrains similar observations by Cassini's UVIS. Data collection interrupted by spacecraft slewing for FIC, 7 measurements: 5 uninterrupted and 2 with interruption for FIC.
	1.2 Abundance of H_2, Cl, Si, O indicative of redox state of Enceladus's interior. Further characterizing the abundance of these materials would constrain the salinity, redox state, and pH, which would further identify synthesis mechanisms that are possible in Enceladus's ocean. This work would help identify the reaction conditions the organics are exposed to.	*m/z* ratios for H_2, further constraining [3]. UV spectra of plume material to constrain pH, redox behavior and salinity [4].	**MS** *Range:* 1-200 amu *Resolution:* >10,000 m/Dm *Min. collector area:* 10x10 cm	**MASPEX** (MS) *Range:* 1-1000 amu *Resolution:* >30,000 m/Dm	
			UVS *Range:* 56-180 nm *Resolution:* 0.3 nm (point source)	**P-ALICE** (UVS) *Range:* 47-188 nm *Resolution:* 0.3 nm (point source) *FOV:* 2x2 deg *iFOV:* 0.27 deg	
2. Determine whether Enceladus's plume material is supplied directly from the ocean or if it interfaces with other reservoirs within the ice shell. *Determining whether the composition of Enceladus's plume is the same as its ocean is crucial to interpreting indirect measurements of Enceladus's ocean.* *Identifying the location(s) of the plume source and evaluating the transport mechanisms would allow for analysis of (1) if the plume is directly or indirectly derived from the ocean and (2) physical or chemical alteration mechanisms that may occur as the liquid is expelled through the ice shell into space.*	**2.1 Ice shell thickness.** Ice shell thickness would provide insight into how far the plume material must travel to get from the ocean to the surface. Identifying the length of travel clarifies the amount of distillation that may be occurring due to expansion of water as the plume material rises, causing condensation within the conduit/vent [5]. Amount and speciation of volatile trapping within [6] can be better estimated given the depth/pressure of the ice shell.	Contrast in dielectric constant consistent with an ocean/ice shell throughout the SPT [7] up to a depth of 5 km with resolution of 1 km.	**Radar (VHF)** *Range:* 60 MHz; 10 MHz bandwidth *Vertical resolution:* 15 m	**REASON** (IPR) *Range:* 60 MHz; 10 MHz bandwidth *Vertical resolution:* 15 m	Instruments pointing nadir. **Radar (VHF):** 4 flybys, radar observations lower than 50 km altitude. **Imager:** 2 flybys, camera must be adaptable to poor illumination conditions of SPT at higher phase angles.
	2.2 Distribution, shape, width, and length of plume vent conduits/fractures within the ice shell. Plume vent conduit/fracture distribution, structure, and depth into the ice would provide insight into the mechanism behind the transport of plume material and ultimately determine whether the vents are directly supplied from the ocean or from within the ice shell (e.g., water lenses, tectonics [8,9]).	Radargrams capable of resolving fractures/conduits length ≤ ice shell thickness. Diffuse radar reflectivity in regions of dielectric contrasts for detecting zones of plume vents.	**Radar (VHF)** *Range:* 60 MHz; 10 MHz bandwidth *Vertical resolution:* 15 m	**REASON** (IPR) *Range:* 60 MHz with 10 MHz bandwidth *Vertical resolution:* 15 m	
		Distribution and size of fractures on surface as indicated by imagery to 1 km scale. Spatial correlation of dielectric constants at depth with spatial position of vents to 1 km scale [7].	**Imager** *Spatial resolution:* ~50 m/pixel *iFOV:* 0.001 rad *Temporal range:* 2 observational periods/flyby *Temporal resolution:* 10 s (min)	**Dawn Framing Camera** *Spatial resolution:* ~50 m/pixel at 535 km altitude *FOV:* 0.096 rad *iFOV:* 93.7 μrad *Focal length:* 150 mm	

Figure 2. Science traceability matrix for Tiger mission concept. The mission has one overarching goal and two associated science objectives. These objectives drive mission and instrument requirements. (a) Projected performance from instrument analogs. Acronyms: MS—mass spectrometer; UVS—ultraviolet spectrograph; SP—south pole/polar; SPT—south polar terrain; SOs—solar occultations; StOs—stellar occultations; FIC–framing imaging camera; IPR—ice-penetrating radar; FOV—field of view; iFOV—instantaneous field of view; UVIS—ultraviolet imaging spectrograph (on Cassini); VHF—very high frequency. References: (1) Postberg et al. (2018b); (2) Waite et al. (2004); (3) Postberg et al. (2009); (4) Hendrix et al. (2015); (5) Glein et al. (2015); (6) Bouquet et al. (2015); (7) Čadek et al. (2016); (8) Kite & Rubin (2016); (9) Porco et al. (2014).

These objectives are informed and focused by discoveries from Cassini and are designed to better understand and constrain the habitability of Enceladus. Cassini carried two mass spectrometers as part of its payload, the cosmic dust analyzer (CDA) and the ion neutral mass spectrometer (INMS). Cassini was able to detect ice and non-ice materials in the form of grains in the plume and Saturn's E ring during its flybys (Porco et al. 2006; Spahn et al. 2006). It also identified organic and inorganic materials in the vapor of the plume via INMS (Waite et al. 2006, 2009). The resulting data did not definitively identify all of the specific organics owing to the lack of resolution and did not investigate high molecular weight organics within the plume. Identifying these organic compounds would allow Tiger to not only catalog products of reactions but also identify precursors for important prebiotic reactions, like amino acid synthesis.

Three types of ice grains were identified and categorized by the CDA on Cassini (Srama et al. 2004): "Type I" are nearly pure water ice grains, "Type II" contain organic compounds (Khawaja et al. 2019) and/or silicates, and "Type III" are more massive in size, as well as rich in sodium and potassium salts. Organic carbon (small carbon-based compounds; e.g., methane), CO_2, HCN, and NH_3 have been detected in the plume vapor with INMS (Waite et al. 2009), although many of these compounds have not been definitively identified at this time. It has even been hypothesized that heteroatom-containing organic molecules are present in the plume; however, more data with a higher-resolution mass spectrometer would be needed to confirm (Magee & Waite 2017; Khawaja et al. 2019). Sodium and potassium (Postberg et al. 2009, 2011), as well as H_2 (Waite et al. 2017, 2009), have also been detected in the plume by Cassini. Detection of sodium-salt-rich ice grains (Postberg et al. 2009, 2011) in the plume suggests that they formed as frozen droplets from a liquid water reservoir in contact with rock, implying rock−water interactions in regions surrounding Enceladus's core (Zolotov 2007; Choblet et al. 2017; Hsu et al. 2015). Understanding the dynamics of Enceladus's plume formation is critical to the interpretation of plume composition as representative of the subsurface ocean. In this mission concept we seek to better constrain and expand on these results. We specifically focus on the presence of organics in the vapor as opposed to within the ice grains.

To address Objective 1, Tiger would definitively identify volatile and semivolatile organic compounds present in the vapor of the plume, as well as determine whether any higher-mass complex organics (100 amu or greater) are present. Specifically, Tiger would be interested in detecting and identifying compounds that can be used as the building blocks of life or to synthesize biological molecules, including carboxylic acids (acetic acid), alcohols (methanol, ethanol), simple amines, and other small volatile organic compounds. All of these examples could act either as starting materials or as products in a variety of prebiotic chemical reactions. Simple organic compounds can be synthesized both biotically and abiotically (Ménez et al. 2018; Barge et al. 2020; Klenner et al. 2020b). The goal of Tiger would not involve determining how these organics are synthesized (i.e., biotically or abiotically), but simply cataloging their presence. A high-resolution mass spectrometer would be capable of identifying the presence of these materials. In order to detect any complex organic structures, the range of the mass spectrometer will include the range previously sampled by Cassini in order to better constrain and identify the organics, but it will also require a higher detection limit to include the possible identification of not only higher-mass volatile materials but also amino acids and nucleobases, as well as any oligomers (1–500 amu). While the larger organics listed will likely not volatilize easily, we determined that it was important to expand our mass range to identify higher-mass volatile species. For physical parameter 1.2, a mass range of 1–200 amu would be required to examine the hydrogen present, as well as to search for any ions in the vapor. While the ions would not likely volatilize, we sought to include a range where they would be detected. A mass resolution of 10,000 m/Dm would be required to distinguish between and identify different compounds. A resolution of 10,000 m/Dm is commonly considered to be "high resolution" for identifying organic compounds (Ramanathan & Korfmacher 2016). The mass spectrometer requires an aperture (at least 10×10 cm area) to collect material from the plume.

For Objective 1.2, the abundance of ions (such as Na^+, Ca^{2+}), H_2, and silicate, previously detected by Cassini (Postberg et al. 2009; Hsu et al. 2015; Waite et al. 2017), would be measured in order to better understand the redox chemistry of the ocean and the conditions the organics are exposed to. This objective would be addressed with two physical parameters: through mass spectral analysis of organic compounds and H_2 (Figure 2, physical parameter 1.1) and UV spectral analysis of sulfur (S: 180.73 nm), silica (Si: 184.55 nm), and other species (Figure 2, physical parameter 1.2). The range and resolution of the UV would need to be 56–180 nm and 0.3 nm, respectively, in order to successfully measure the distribution of the ions. This range and resolution is based on previous work where atomic species such as Cl, O, and Si were successfully measured (Cook et al. 2013).

To address Objective 2, understanding the transport of material from the subsurface ocean through the ice shell requires knowledge of the ice shell's physical properties. While topography and gravity measurements collected during the Cassini mission suggest that a subsurface ocean exists (Iess et al. 2014; Čadek et al. 2016; McKay et al. 2018), more information is required to fully understand the interaction between the ocean and the ice shell. These include the distribution, width, shape, and length of the plume vent conduits and fractures within the ice shell. Knowledge of these physical parameters will determine whether the plume is directly sourced from the ocean or from reservoirs within the ice shell itself (Kite & Rubin 2016). Determination of vent structure through the ice shell can additionally determine whether processes such as distillation (Glein et al. 2015) may be occurring as the material ascends through the shell by constraining the length of time of transport and partial pressures throughout the vent conduit. By determining the transport mechanisms of the plume from the source of the material to expulsion external to Enceladus, the compositional measurements can be better understood and the reliability of the plume as a direct analog to the interior ocean composition can be established. These properties are determined through measuring the dielectric constant in the subsurface to constrain ice thickness using radar sounding. Resulting radargrams collected in the south polar terrain (SPT) region, when correlated to surface features from imaging, will help characterize the ice shell thickness and subsurface structures of the tiger stripe fractures to assess the connectivity of the ocean to the surface. Multiple radargrams collected over the length of the mission will help assess spatiotemporal variability of subsurface features in the SPT in three dimensions. To resolve features of interest within the tiger stripe region, the ice-penetrating radar will be in the very high frequency (VHF) band in the 60 MHz range. The imaging system will require a spatial resolution of $\sim$50 m pixel^{-1} to sufficiently resolve surface features at comparable resolutions produced by the radar soundings. Two imaging periods per flyby for the first two flybys would be required for stereophotogrammetry.

3. Payload

Tiger's instrument payload will permit in situ analysis of the plume vapor and remote sensing of the surface and interior of Enceladus. The suite consists of a mass spectrometer, ultraviolet imaging spectrograph, single-band ice-penetrating radar, and imaging camera (Table 1). For this study, analog instruments have been chosen to constrain science and engineering requirements for Tiger. These instruments would require specific modifications for operation in the Enceladus environment, but adapting these instruments was beyond the scope of this study. All instrument analogs are based on hardware that has either previously flown or been selected for upcoming missions. Each instrument analog, the physical parameters they will measure, and the science objective requirements they satisfy are summarized in Table 2.

3.1. Mass spectrometer Analyzing Water vapor (MAW)

The analog for our mass spectrometer, the Mass spectrometer Analyzing Water vapor (MAW), is a modified version of Europa Clipper's MAss Spectrometer for Planetary EXploration (MASPEX; Brockwell et al. 2016). MAW would be used to address the science questions in Objective 1. The flyby altitude at which MAW would analyze the plume vapor is in the range of 20–50 km, in order to successfully collect adequate amounts of sample and not destroy organic material (Klenner et al. 2020a). While Klenner et al. address the impact of ice grains, gas-phase organics will likely fragment as well. MAW would have a much higher resolution than INMS, which would give higher-resolution spectra to differentiate organics with similar masses. MASPEX is designed to be able to determine the different isotopes of simple organics and water (Brockwell et al. 2016). In addition, MAW would also be able to measure complex organics that Cassini was unable to, which will give more information about complex organics present in the vapor of the plume. The range on Cassini's INMS was 1–100 amu (Postberg et al. 2018a), compared to 1–1000 amu for MAW, which would allow it to adequately address Objective 1.

Table 1
Instrument Table Describing the Current Best Estimates (CBE) for Tiger's Analog Instrument Suite

Payload Accommodation Requirements	MAW—Mass-spec Analyzing Water Vapor	ROAR—Ridge and Ocean Analyzing Radar	CUB—Charge Transfer Ultraviolet Band Imager	TAIL—Topography Assessment Imager for Enceladus's Lithosphere
	Mass Spectrometer	Radar	Ultraviolet Spectrograph	Imaging System
Analog	MASPEX	REASON (VHF band only)	P-ALICE	Dawn Framing Camera
CBE mass (kg)	30	50.8	4.4	5.5
CBE power (W)	14 (peak) 8.0 (standby) 4.5 (survival)	37 (in operation) 42 (in warm-up) <1 (survival)	4.5 (peak) 4.2 (standby) 4 (survival)	17 (in operation) 15 (in warm-up/standby) <1 (survival)
CBE peak data rate (s) (bps)	57,000	80,000,000	4,000	12,000,000
Viewing direction in body coordinates	Ram	Nadir	Nadir	Nadir
CBE dimensions ($L \times W \times H$ in m)	$0.4 \times 0.2 \times 0.05$	Two antennas: $3 \times 0.15 \times 0.15$ Electronics: $0.35 \times 0.25 \times 0.20$	$0.44 \times 0.16 \times 0.12$	$0.14 \times 0.23 \times 0.1$

References. Mass spectrometer (Brockwell et al. 2016), single-band ice-penetrating radar (Blankenship et al. 2009), ultraviolet imaging spectrograph (Stern et al. 2008), and imaging camera (Sierks et al. 2011).

Scaling of mass from the MASPEX baseline was based on personal communication with the Europa Clipper payload team. Based on this discussion, MASPEX components that were driven by Jupiter's radiation environment (e.g., harness, cooler, and shielding) were removed for MAW, given the less intense radiation in the Saturn system, resulting in a final mass of 30 kg.

3.2. Charge-transfer Ultraviolet Band spectrograph (CUB)

The analog for our ultraviolet imaging spectrograph, the Charge-transfer Ultraviolet Band spectrograph (CUB), is P-Alice, a UV imaging spectrograph, currently part of the Persi suite on the New Horizons mission. The Alice family of UV spectrographs are lightweight (4.4 kg), low-power (4.5 W) instruments ideal for imaging ion species with stellar and solar occultations (Stern et al. 2008). Previous iterations of Alice have been included as payloads on missions such as New Horizons, Juno, and the Lunar Reconnaissance Orbiter, making this a robust UV instrument for occultation observations of ion species at Enceladus's south pole (Stern et al. 2008; Gladstone et al. 2017, 2010). P-Alice has a bandpass of 47–188 nm with a spectral resolution of 0.3 nm and a slit designed to be used for both stellar and solar occultations. To tailor P-Alice for our mission, we propose that CUB should include an aperture door that will close for the duration of the south pole plume fly through (where material would be sampled for analysis via MAW), in order to reduce collection of plume debris on the instrument and allow for successful collection of data.

3.3. Ridge and Ocean Analyzing Radar (ROAR)

The analog for our ice-penetrating radar, the Ridge and Ocean Analyzing Radar (ROAR), is the Radar for Europa Assessment and Sounding: Ocean to Near surface (REASON), an ice-penetrating radar that will be included on the Europa Clipper mission. To reduce mass and power usage, our design would utilize the VHF band in the 60 MHz range. Scaling of mass and power from REASON's baseline after removing the HF band was based on personal communication with the Clipper payload team, which led to a decrease in mass of 40% and power of 25% (Table 1). While the data volume collected would be relatively large, the aggregate data collected for mapping desired features are appropriate. The radar would operate with a bandwidth on the order of tens of MHz to acquire a vertical resolution of tens of meters. The signal loss through the ice will depend on the temperature profile of the ice, the amount of impurities, and porosity of the ice. The VHF on REASON operating at 60 MHz with bandwidth of 10 MHz is required to sound a minimum of 4.5 km depth in the ice shell (West et al. 2017) and is expected to exceed this requirement, which is inclusive of a number of estimates of Enceladus's south pole ice shell thickness. However, due to colder ice temperatures and potentially lower salinity in the ice shell at Enceladus, there will likely be less attenuation in the Enceladus environment, which could allow for measurements of deeper ice–ocean interfaces using VHF than at Europa. The primary limitation to depth of sounding for the VHF is surface scattering, which is more pronounced for shorter-wavelength radar. Selecting a narrower bandwidth (longer wavelength) would increase the signal. An expanded discussion on measurement of the depth of the ice shell using radar can be found in Section 6.4. The horizontal, or azimuthal, resolution will be on the order of a few hundred meters, which is less than the estimated width of the tiger stripes, which have an average width of 2 km (Porco et al. 2006). In addition, the azimuthal resolution would be high enough to detect bodies of water, as well as any additional tectonic processes within the ice shell (Blankenship et al. 2009). The radargrams will be collected perpendicular to the tiger stripes. Advanced synthetic aperture radar (SAR) processing would need to be performed, to reduce the impact of diffuse and volume scattering to achieve higher signal-to-noise ratio (Blankenship et al. 2009).

3.4. Topography Assessment Imager for Enceladus's Lithosphere (TAIL)

The analog for our imager, the Topography Assessment Imager for Enceladus's Lithosphere (TAIL), is the Dawn mission Framing Camera, which has both acceptable capability and favorable size, weight, and power characteristics. Images

Table 2
Tiger's Science Objectives and Physical Parameters Mapped to the Instrument Payload

Science Objective	Physical Parameter	Mass Spec	Radar	UV Spec	Camera
1. Determine whether Enceladus's volatile inventory undergoes synthesis of complex organic species that are evidence for a habitable ocean.	1.1 Determine whether key building blocks for life exist in Enceladus's ocean	✓			
	1.2 Abundance of H_2, Cl, Si, O indicative of redox state of Enceladus's interior	✓		✓	
2. Determine whether Enceladus's plume material is supplied directly from the ocean or if it interfaces with other reservoirs within the ice shell.	2.1 Ice shell thickness		✓		✓
	2.2 Distribution, shape, width, and length of plume vent conduits/fractures within the ice shell		✓		✓

from TAIL would be primarily used for scientific context and correlation with subsurface features detected by ROAR. Imaging periods would occur both on approach to and on departure from the closest pass over the SPT for the first two flybys. With an iFOV of 93.7 μ rad (Sierks et al. 2011), TAIL would nominally image the SPT from an altitude of 535 km at a resolution of 50 m pixel^{-1}. Six images would be taken during each imaging period to cover topographic areas of interest. Higher-resolution images can be obtained by imaging at a lower altitude, though more images would be needed to cover the same surface area. Ground sampling distances finer than 10 m pixel^{-1} would be achievable at closest approach, though such resolution is not necessary to achieve the stated science objectives.

4. Mission Architecture

The architecture of the Tiger mission concept has been designed using the JPL Team X concurrent engineering process, taking into account NF-class constraints and the science priorities identified in the concept design process. The full NF5 AO has not yet been released as of the completion and submission of this work, so notional NF limits based on previous AOs (Niebur 2016) and expectations for the future one have been used in the design of this mission concept. Systems have all been designed to meet a NASA class B risk classification with appropriate redundancies included throughout. NASA risk classification levels determine acceptable mission risk posture depending on how critical each mission is to NASA's Strategic Plan (NASA 2004); the OSIRIS-REx NF mission is also a Class B mission (Leitner 2014).

4.1. Mission Trajectory and Timeline

Tiger would launch in 2029 June with $C_3 = 14.3$ km^2 s^{-2} and utilize a Venus–Earth–Earth gravity assist trajectory (to reduce fuel mass) to arrive at Saturn in 2038 March (Figure 3). The interplanetary cruise time would be 8.8 yr, the orbit adjustment time after Saturn orbit insertion would be 0.8 yr, and the science phase would be 1.2 yr. During the science phase, Tiger would remain in Saturn orbit and fly by Enceladus every 62 days. Seven flybys of Enceladus would provide enough data to fulfill our science objectives, and an additional contingency flyby is also included, for a total of eight flybys. At the conclusion of the mission (2040 February), the spacecraft would be disposed of into Saturn. The total change in velocity performed by the spacecraft (total ΔV) throughout the mission would be 2.185 km s^{-1}. Because ΔV can be related to necessary fuel mass through the rocket equation, this is used to estimate total fuel mass needed to complete the mission.

4.2. Configuration

The Tiger spacecraft was designed to be reliable, fit inside of the launch vehicle, and complete the science objectives. There would be limited moving parts, primarily the reaction wheels for spacecraft attitude control and the radar antenna requiring a one-time deployment. An Atlas V 431 rocket with a 4 m extended payload fairing (XEPF) would be used to launch the 2410 kg spacecraft. Figure 4 (left) illustrates Tiger's stowed configuration inside of the launch vehicle. The base of the cylindrical bus contains the main engine (100 lbf HiPAT, similar to an engine used on Cassini; Barber 2018), four thrusters, and two next-generation (Next-Gen) radioisotope thermoelectric generators (RTGs) covered by two RTG Sun shields for protection during the Venus flyby. The RTGs are mounted to the base of the spacecraft (similar to Cassini; Gordon & Kern 2015) and balanced 180° apart. Above the engine and the RTGs, the spacecraft is split into two modules: (1) a propulsion module containing propellant tanks and reaction wheels, and (2) an avionics module containing batteries, attitude sensors, electronics, and instrumentation (Figure 4, right). Finally, a 2.7 m high-gain antenna (HGA) for telecommunications is mounted to the top of the spacecraft. Three of the instruments are mounted in the nadir pointing direction (Table 1), and their view is unobstructed during a flyby of Enceladus (Figure 5).

The maximum expected wet (launch) mass of 2410 kg results in a wet mass margin of 62% considering that the estimated maximum launch vehicle capability is 3915 kg for Tiger's interplanetary trajectory. The maximum expected wet mass includes a total contingency mass of 43%; 22% (182 kg) of the total contingency mass is allocated on a per-subsystem basis, while 21% (167.6 kg) is allocated system wide. Full details of subsystem masses and contingencies are included in Table 3.

4.3. Power

The design of the power system is constrained by the power requirements from the science instruments, spacecraft subsystems, and the distance of the spacecraft from the Sun. A solar array power architecture was considered impractical owing to low solar irradiance at 9.5 au and would likely exceed the mass constraints of the spacecraft. Next-Gen RTGs were selected for the radioisotope power system (RPS) following a trade study between multimission radioisotope thermoelectric generators (MMRTGs), enhanced MMRTGs (eMMRTGs), and Next-Gen RTGs, due to their very high power output at the end of life and low annual power degradation. Advancements in the thermoelectric couple efficiencies have shown promise toward the development of Next-Gen RTGs. The Next-Gen RTGs are based on three concepts: Segmented RTG (SRTG), the Segmented-Modular RTG (SMRTG), and the Hybrid-Segmented Modular RTG (HSMRTG) (Matthes et al. 2018). The SMRTGs can be produced in eight variants between 2 and 16 General Purpose Heat Source (GPHS; Woerner 2018). The selected Next-Gen RTG variant for our study is SMRTG with 8 GPHS. The spacecraft configuration would require two units of 8 GPHS Next-Gen RTG, which can produce 326 W of total power output at the end of mission. A 10 Ah Li-ion battery system would be included to accommodate the peak power requirements and ensure that the power balance would be positive for the duration of the mission. Additional details on the power system are included in Section 6.7.

4.4. Thermal

The thermal subsystem of Tiger needed to be designed so that all components in the spacecraft would remain within operational or survivable temperature levels in both the cold environment of the outer solar system and the hot environment in the vicinity of Venus, where a flyby will be performed. Multilayer insulation (MLI) would enclose the spacecraft to avoid excessive heat transfer to and from the outside environment, providing better thermal stability and control. When the spacecraft would be <1 au from the Sun, the HGA

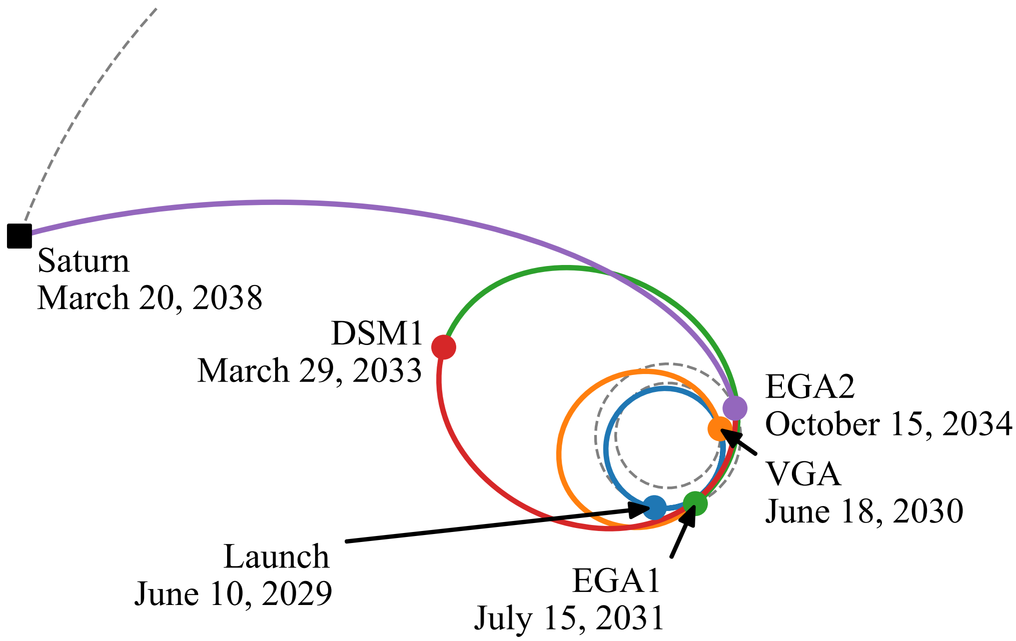

Figure 3. Proposed Tiger interplanetary trajectory from Earth to Saturn, where VGA stands for Venus Gravity Assist, EGA stands for Earth Gravity Assist, and DSM stands for Deep Space Maneuver.

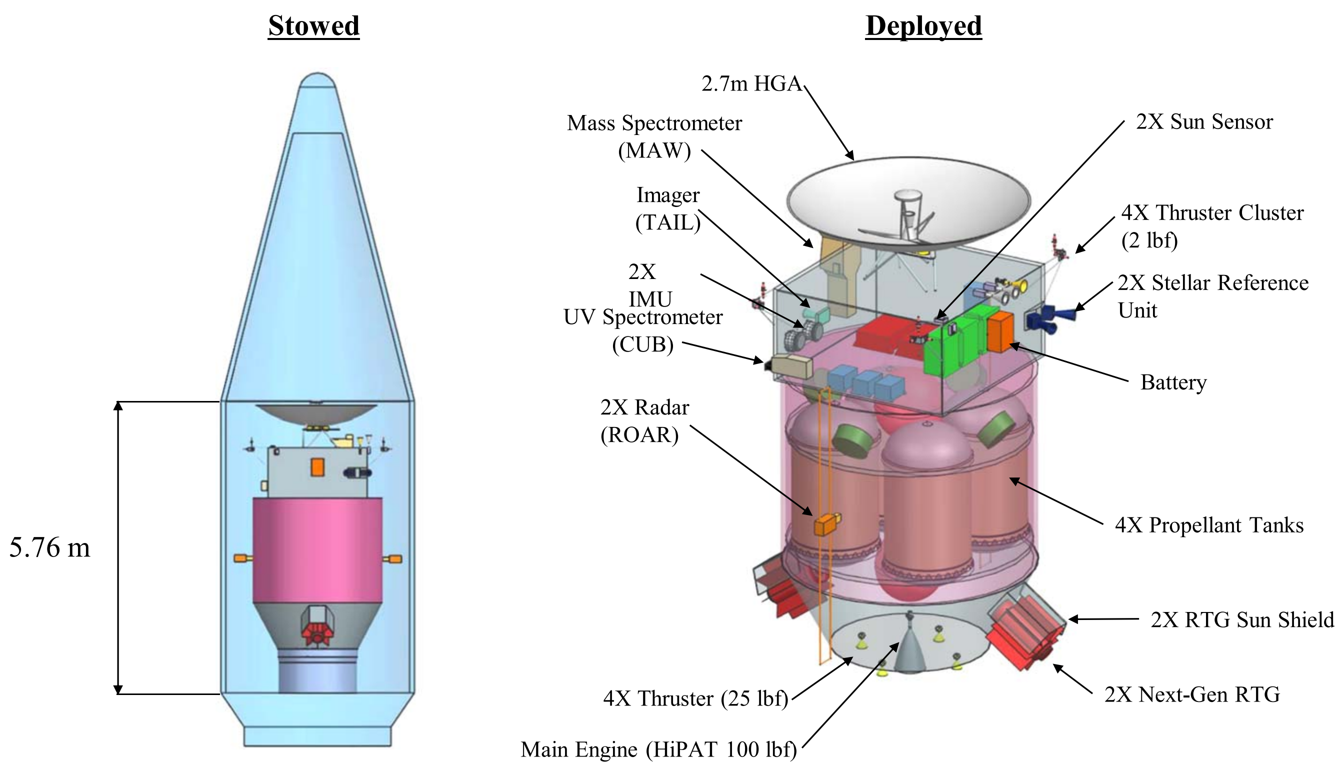

Figure 4. Tiger launch configuration (left) and instrument locations (right).

would be pointed toward the Sun to shield the spacecraft from direct solar radiation. Radiators would also be used along with a pumped fluid loop for the hot case to ensure that excessive heat is radiated out. For the colder case in the outer solar system, the spacecraft would use waste heat from the RTGs to keep itself warm. Not only would the RTGs be partially located inside the MLI to passively provide heat, but also the pumped fluid loop would be used to transfer this waste heat from the RTGs to the propellant tanks and electronic components. This is in conjunction with 30 strategically placed Radioisotope Heater Units (RHUs) used to keep various components warm. A pumped fluid loop is more expensive and has been used fewer times in space missions compared with electric heaters, but it consumes significantly less power, as it leverages the waste heat from the RTGs to keep the spacecraft warm. Electric heaters, on the other hand, would consume more power than

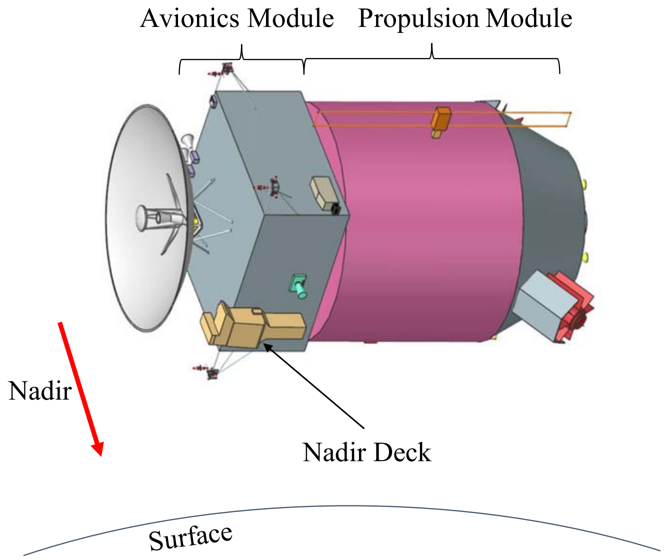

Figure 5. Tiger science flyby configuration.

what could be produced by the power subsystem to keep the propellant and electronics above their threshold temperature. The need for a more efficient power management, combined with a large margin in the budget, culminated in the selection of the pumped fluid loop strategy for our spacecraft.

4.5. Propulsion

Tiger's propulsion system would leverage commercially available hardware with flight heritage and have built-in redundancies to ensure the success of the system. A single Aerojet R-4D-15HiPAT, which is capable of delivering 100 lbf of thrust, would serve as the main engine. Tiger would also utilize four Aerojet R-1E engines for trajectory control, which, when fired simultaneously, could also generate 100 lbf of thrust and serve as a backup to the main engine. Tiger would also include 12 MOOG Leros LTT engines for attitude control. All engines would be bi-propellant, using monomethylhydrazine (MMH) as fuel and nitrogen tetroxide (NTO) as their oxidizer. Propellant would be fed to the engines using a blow down feed system using helium as a pressurant. The oxidizer and fuel sides of the feed system would each be broken up into two parallel lines (using a mix of latch, solenoid, and pyrotechnic valves), to ensure feed system performance in the event of a valve failure.

4.6. Attitude Determination and Control Systems

The attitude control design would include four Collins Teldix reaction wheel assemblies (RWAs) for control in a pyramid configuration, two orthogonal Sodern Hydra star trackers, two Adcole coarse Sun sensors opposite the instruments, and two Honeywell miniature inertial measurement units (MIMUs) for attitude determination (Wie et al. 2014; Carson et al. 2016). All duplicates are backups, and attitude control performance is tolerant to one failed reaction wheel through pyramid placement of the RWAs. Momentum management would be performed through desaturation from thrusters outside of science windows to provide high precision and accuracy during science observations. Science requirements do not necessitate ground post-processing of navigational attitude data. Overall, the attitude and determination control system design would not be particularly challenged by science requirements, which are relatively forgiving to pointing knowledge and control requirements, so the primary design concern is redundancy for the long-duration mission.

4.7. Command and Data Handling

Tiger would nominally use the Next-Gen Sphinx command and data handling system (Imken et al. 2017). This system can store 12× the volume of science data that is collected during each Enceladus flyby and can handle the differing data rates from each science instrument. The Sphinx system has been developed as a miniaturized, radiation-hardened system designed specifically for deep space Cubesat missions. It will be used for the Lunar Flashlight and NEA Scout missions, which have not yet launched as of this writing. The Tiger mission is longer in duration and travels farther from Earth than the Lunar Flashlight and NEA Scout missions, so it is possible that the Sphinx system may not be adaptable to the increased demands. However, if necessary, a more conventional system for deep space missions can be used without impacting the feasibility of Tiger; the more conventional system would require more mass and power but would not adversely impact the ability to achieve Tiger's science goals.

4.8. Telecommunications

Tiger would utilize the Deep Space Network (DSN), which has enabled interplanetary communications, for its data downlink, telemetry, and communications. This design would include a fully redundant *X*-band subsystem, downlinking at 7.3 kilobits per second (kbps) and uplinking at 2 kbps at the maximum expected solar distance of 11 au. The 62-day period between Enceladus flybys would provide ample time to downlink data from each pass, and science data could be downlinked without use of a *Ka*-band system. The telecommunication subsystem has been designed with $\geqslant 3$ dB link margin.

4.9. Ground Systems

Tiger would utilize the DSN and Mission Support Area at JPL with standard Advanced Multi-Mission Operations System tools to manage mission operations. Because each successive flyby would not be reliant on analyzing data from the previous one, we would be able to simplify our mission operations with preplanned sequence commands to the spacecraft. Given the amount of data collected during each Enceladus flyby, the total downlink time is <15% of the spacecraft orbital period about Saturn. This communication would nominally split into 4 hr downlink times each Earth day, and full downlink would be completed before the next flyby. Therefore, a 34 m beam waveguide antenna would be sufficient to support the downlink capability necessary for this mission. Once the data are on the ground and processed, they would be delivered to the Planetary Data System archive and made available to members of the scientific community.

Table 3
Subsystem Mass Values

System	Mass Fraction (%)	Current Best Estimate (CBE) Mass (kg)	Contingency (%)	CBE + Contingency (kg)
Instruments	11	90.7	28	116.4
Attitude control	5	41.9	10	46
Command and data	1	8.3	17	9.7
Power	11	91.9	24	113.7
Propulsion	16	131.6	6	139.1
Structures	33	268.5	28	343.7
Cabling	6	51.8	30	67.4
Telecommunications	6	47.3	14	53.7
Thermal	10	81.2	30	105.6
Total dry mass	100	813.2	22	995.3
System contingency (kg)		167.6		
Propellant (kg)		1247.6		
Launch mass (kg)		2410.4		

5. Cost

The total cost of the Tiger mission was estimated to be $636 million USD in FY22 with a reserve of $363 million USD for the $999 million USD budget cap of the NF4 AO. JPL's Institutional Cost Model (ICM) was applied to estimate the development and production costs of the spacecraft. ICM is a hybrid parametric/analogy cost model based on previously flown missions that calculates the specific NASA Work Breakdown Structure (WBS) elements based on specific mission and vehicle design traits using Cost Estimating Relationships or "wraps." Tiger's WBS is detailed in Table 4. WBS 1 and 2 were estimated based on the scope and class of the mission. WBS 3 was estimated using an ICM relationship relating radiation dosage, duration of phases, and other traits. WBS 4 estimation included relationships between scientific objectives and instrument models. Instrument cost (WBS 5) was estimated using the NASA Instrument Cost Model (Mrozinski 2018). The spacecraft costs were estimated using triangular distribution to relate the historical cost estimates within ICM to an "Out of House" procurement strategy including development and production (WBS 6), as well as integration and test (WBS 10). There is no cost value in WBS 10 for Project Systems and Integration and Testing, as this is accounted for in WBS 6 through the JPL ICM Triangle Distribution for cost estimation. The Mission Operation System (WBS 7) and Ground Systems (WBS 9) were estimated based on technical parameters relating to analogous missions. One of the assumptions of the NF4 AO is that the launch cost for a selected mission is provided by NASA and is not part of the total mission budget (WBS 8), and we assume that NF5 will maintain similar standards. Given the total cost, the reserves for this mission are approximately 57%, which hedges some of the technological challenges of this mission, described in Section 6. Additionally, the total cost estimate for Tiger falls under the advanced announcement of the $900 million (FY22) USD NF5 cost-cap estimate. Therefore, we believe that any changes to either cost-cap or design architecture could be reasonably accommodated to either NF4 or NF5 cost caps with Tiger's considerable cost reserves. The cost estimate exercise for Tiger was performed to demonstrate that the final architecture decided on would fit within the budgetary constraints of an NF-class mission. There are inherently many uncertainties associated with costs related to both the instrument payload and the spacecraft. These uncertainties would be addressed during the mission's development phase.

6. Trades and Challenges

Designing a deep space planetary science mission is a complex task with a great number of factors to consider. A primary challenge in the design process is iterating on an architecture such that it meets all necessary constraints to be a feasible and selectable mission, while also answering priority science questions posed by the community. Another common challenge for habitability and life-detection focused missions are concerns about contamination and outgassing. For any mission of this kind, a rigorous contamination control assessment in accordance with the planetary protection policies outlined by the international Committee on Space Research (COSPAR) would be necessary. Contamination control is a nontrivial aspect of spacecraft development, but recent work (McKay et al. 2020) has advanced the technology necessary to adequately decontaminate spacecraft for life detection missions with more stringent requirements than habitability missions. In this section we discuss key trade studies performed and challenges encountered in the iterative process of designing Tiger. These ideas are presented to inform the community and aid in future mission development for ocean worlds.

6.1. Selecting Science Goals

Our science objectives focus on habitability to constrain environmental context in order to better equip future life detection missions. This allowed us to remain within NF-class mission constraints, compared to focusing on a mission that would have had more costly life-detection driven objectives. By prioritizing habitability objectives, future life detection experiments can potentially leverage the technology learnings gained to optimize selection of instrument payloads and requirements, as well as scientific objectives that are specific to life detection.

Previous mission concepts that aimed to study the geophysical properties of Enceladus are typically architected to involve in situ exploration or multiple landed seismometers (e.g., Spencer 2010a, 2010b). The fundamental understanding of energy sources within Enceladus has become increasingly important owing to the differing interpretations of the thermal evolution of Enceladus. In addition, an understanding of the

Table 4
NASA Work Breakdown Structure for the Tiger Mission

WBS Element	Cost [A-D] FY22 $M USD
1—Project Management	17.5
2—Systems Engineering	44.1
3—Safety and Mission Assurance	28.5
4—Science	28.4
5—Payload	180.7
6—Spacecraft	282.2
7—Mission Operations	26.8
8—Launch Vehicle/Services	0
9—Ground Systems	27.6
10—Project Systems I&T	0
Subtotal	635.8
Reserves	363.2 (57%)
PI Managed Total Cost	999.0
AO Budget Cap FY22 USD	999.0

rocky mantle structure and porosity can provide knowledge of Enceladus's formation and alteration history. However, we did not choose to explore these and other questions about the interior structure of Enceladus, as they would have best been answered by in situ exploration (Spencer 2010a, 2010b). In addition, the NF4 call for an Enceladus mission specifically solicited a habitability mission, making a purely geophysical mission less compelling from a selection and NF eligibility standpoint.

Life detection mission concepts to Enceladus have been increasingly proposed (MacKenzie et al. 2020). Such concepts require instrumentation with highly specific and repeatable instrument measurements in order to meet standards of detection (Neveu et al. 2018). While such a mission could be considered within NF constraints, there is a high risk of scientific return being inconclusive, and therefore incommensurate with the expectations of an NF mission. These risks could be potentially mitigated through carefully measured planning of mission goals such that scientific return would still be commensurate even with inconclusive life detection results. The Tiger payload is designed with future life detection missions in mind, such that risks associated with instrument selection, range requirements, sensitivity, and reliability can be reduced through contextual knowledge of the habitability environment gained through Tiger's science objectives and goals.

A comparison of Tiger to similar Enceladus mission concepts (Enceladus Life Signatures And Habitability (ELSAH), Enceladus Life Finder (ELF), and Orbilander), as well as the Europa Clipper mission, is included in Table 5. Of the Enceladus concepts, Tiger is the only habitability-focused concept without explicit life detection objectives. Europa Clipper is also a habitability-focused mission with no explicit life detection requirements or objectives. The Tiger mission concept assumes that a life detection mission could follow later with instruments and objectives specifically designed around life detection. Similarly, the proposed Europa Lander could follow Europa Clipper's habitability-focused mission to achieve life detection objectives. The instruments used to obtain these habitability and life detection objectives vary widely among concepts, with the exception of mass spectrometry.

6.2. Orbiting versus Flyby Mission Architecture

An Enceladus-orbiting mission architecture was initially explored to answer a larger number of science questions compared to a flyby mission, given that an orbiting mission would have improved access to Enceladus. However, an orbiting mission was found to likely exceed the cost, mass, and power limits associated with an NF-class mission. One of the challenges of the orbiting architecture was balancing flight time, propellant mass, and RTG lifetime. A significant amount of propellant would be needed to enter Enceladus orbit, which would increase cost, launch mass, and requirements on other spacecraft subsystems (e.g., increased power requirements to maintain more fuel at liquid temperatures). While total flight time could be increased to reduce the propellant mass, RTGs have finite lifetimes that limited the amount of mass reduction that could be realized. Further, providing enough power for frequent data collection and communication back to Earth in an orbiting mission was also a significant challenge. Such problems are representative of the barriers encountered during the design of an orbiting mission but were not the only issues found. These considerations led us to select a flyby mission architecture that would have fewer opportunities for science but would be possible within NF constraints. Further, we found that a flyby architecture, despite having fewer scientific opportunities, would still support scientific data collection commensurate with an NF-class mission. The final mission architecture would incorporate seven flybys as the baseline for collecting sufficient scientific data. Mission designs like ELF have incorporated 10 Saturn orbit flybys of Enceladus with the aim of collecting a culmination of plume-related organics with instruments of higher resolution (Reh et al. 2016).

6.3. Instrument Selection

Several instruments were initially considered for inclusion in the science payload for the purposes of a habitability mission. These included ice-penetrating radar, UV spectrograph, mass spectrometer, microwave/submillimeter radiometer, laser altimeter, and imaging camera. All of the considered instruments were a combination of remote sensing and in situ instruments, as a landed mission architecture was not considered in this study owing to NF cost constraints.

To obtain compelling science that met the standards of an NF-class mission and would provide data beyond those already obtained by Cassini, instruments that could provide further insight into the south polar plume composition and origin were given priority. One instrument that stood out in this regard was a mass spectrometer, which could further constrain the types and abundances of organics detected by Cassini. Identifying these organics can provide critical clues about the processes and chemistry of the interior of Enceladus. While Cassini carried two mass spectrometers, we chose to only carry one mass spectrometer in order to vary our payload and address multiple science objectives. In this study, we focused on analyzing the volatiles and semivolatiles within the vapor rather than within the ice grains. The mass spectrometer would require a minimum aperture of a 10×10 cm area to collect material from the plume. In the future, additional trade studies during mission design would address varying aperture sizes (e.g., to an area of 1 m^2 for the collector) with sampling at different flyby altitudes in the range of 20–50 km of the plume. While this could not be investigated during the Team X

Table 5
Comparison of Tiger to Similar Mission Concepts

	Tiger	**ELSAH**	**ELF**	**Clipper**	**Orbilander**
Mission Class	New Frontiers	New Frontiers	New Frontiers	Flagship	Flagship
Target body	Enceladus	Enceladus	Enceladus	Europa	Enceladus
Architecture	Flyby (Saturn orbiting)	Unknown. Information not publicly available	Flyby (Saturn orbiting)	Flyby (Jupiter orbiting)	Orbiter + lander
Mission goal	Habitability	Habitability & life detection	Habitability & life detection	Habitability	Life detection
Instrument payload	Mass spectrometer, radar, UV spectrograph, camera	Unknown. Information not publicly available	Mass spectrometer, dust analyzer	TIR, NIR, and VIS imaging spectrometers, UV spectrograph, radar, magnetometer, magnetic sounder, mass spectrometer, dust analyzer	Seismometer, microscope, sequencer, mass spectrometer, cameras, laser altimeter, radar

Reference. Europa Clipper (Phillips & Pappalardo 2014), ELF (Reh et al. 2016), ELSAH (Eigenbrode et al. 2018), and Orbilander (MacKenzie et al. 2020).

mission concept study, this consideration would provide more quantitative constraints for the payload architecture (Guzman et al. 2019; Neveu et al. 2020). With Tiger's considerable cost reserves, the result from such a trade study could allow for modifications to be made to the payload during mission development. At a minimum, Cassini was able to detect material under similar conditions, and Tiger seeks to detect organics at the concentration of the dissolved organic carbon in the ocean.

The other instrument that could provide complementary insights into Enceladus's interior was the ice-penetrating radar. Ice-penetrating radar could provide glimpses into the interior by gaining clues into the plume's origin, which could not otherwise be determined without a more costly landed mission. Both of these instruments are relatively massive (in volume and weight) and take up a considerable amount of the payload cost.

In conjunction with the mass spectrometer and ice-penetrating radar, an imaging camera was considered next most critical to meeting mission objectives. An imager could provide additional surface context and supplemental topography and calibration data for the ice-penetrating radar measurements.

The remaining considered instruments were the UV spectrograph, microwave radiometer, and laser altimeter. Based on estimates of cost and mass, only one of these instruments would fit onto the payload. The laser altimeter, being the largest of the remaining instruments, exceeded cost constraints for the mission. As a tool to gauge tidal topography of Enceladus, the laser altimeter required multiple orbits close to specific periodicity, a frequency that could not be achieved with our chosen flyby via orbit of Saturn. The microwave radiometer was estimated to be the next largest, and initial calculations indicated that it could be feasible on the mission architecture within constraints. This led to the choice between the UV spectrograph and the microwave radiometer to fit onto the payload. The UV spectrograph was ultimately chosen, as it was the smaller of the two and complemented the science goals of the mass spectrometer, while the microwave radiometer did not fit into our science goals as compellingly because it focused on geophysical measurements primarily associated with the surface and not the subsurface or plume source region. The decision was ultimately driven by instrument costs and alignment with our mission goals. An Enceladus mission architecture with different cost constraints or mission goals may benefit from a different science payload than the one selected for Tiger. For instance, a mission with science goals focused on understanding energy sources within Enceladus may find more benefit from a microwave radiometer.

Our instrument analogs fall in the mid−technology readiness level (TRL) range, as do many of the projected ocean world instrument needs (Klenner et al. 2020a; Schmidt et al. 2021). Targeted investment in the advancement of ocean world and life detection instruments and technologies would need to be prioritized over the coming decade to facilitate Tiger's mission timeline. Tiger does, however, have significant cost reserves available to help mitigate this mission risk.

6.4. Ice-penetrating Radar

One of the most important trades considered for the Tiger mission was the inclusion of a single- or dual-band ice-penetrating radar system. While a single-band radar system would be substantially smaller in size and therefore less costly, a dual-band system would provide a higher level of science return.

A dual-band radar, similar to Europa Clipper's REASON radar, would enable measurements of features of different sizes at varying depths within the ice shell. This would be useful for discriminating both smaller, surface, and shallow subsurface features such as the fractures at the SPT, as well as larger, deeper features like the ice–ocean interface. While shorter bandwidths can still potentially reach the ice–water interface, an abundance of surface clutter and reflective features at shallower ice shell depths may reduce return signal at the ice–ocean interface, making it potentially difficult or impossible to detect. In terms of scientific return, dual-band radar would be highly preferential.

The drawbacks to dual-band radar, and therefore the benefits to single-band radar, are the increased mass, power, cost, and data volume required of a dual-band system. The radar on Tiger was adapted to be single-band to meet constraints found in early iterations of the Tiger architecture, where the spacecraft was Enceladus orbiting rather than Saturn orbiting with Enceladus flybys. Because the Enceladus-orbiting architecture required significantly more propellant, less mass was available for the science payload. Frequent radar data collection also contributed to difficulties in communicating data back to Earth in a timely manner. Given that the change to a Saturn-orbiting architecture resulted in large mass and cost margins, it may be possible to use a dual-band radar in place of the single-band radar currently described. Data volume is also less of a concern for the flyby architecture because the number of Enceladus encounters is limited and there is a large amount of time between passes to downlink data. However, further system level analysis would be required in order to both verify that a dual-band radar is technically feasible and decide whether the risk posture of such a mission is desired (i.e., if the reduction in cost and mass reserves is warranted by the science gained by adding the second band). Adding a second radar band could also be considered for a baseline mission requirement, while the threshold requirements could remain based on a single-band radar.

Given Enceladus's estimated ice shell thickness, anywhere from the range of less than 5 km (Čadek et al. 2016) to 30–40 km (Lucchetti et al. 2016), and that its topography (Giese & Cassini Imaging Team 2010) is described to be shallow depressions in the region of interest, the icy subsurface will likely have a higher absorption coefficient the further the radar penetrates. Compared to Europa, Enceladus's likely colder and purely conductive ice shell at the SPT will have lower absorption. Surface scattering, which is believed to be significant at Europa (Blankenship et al. 2009), would likely be similarly challenging to radar at Enceladus. However, radar at Enceladus will have a less challenging noise environment at Saturn as compared to REASON, which will be affected by Jupiter's ionosphere (Blankenship et al. 2009), allowing for a stronger and better echo strength in the Enceladean environment. While further analysis should be done, the variables discussed above would suggest that using a system similar to REASON's VHF will have increased performance at Enceladus, allowing for clearer sounding in the Enceladus ice shell. It is also of note that Enceladus's ice shell at the SPT is believed to be thinning (Nimmo 2020). If true, the base of the ice shell may be smoother relative to an accreting ice shell, allowing for less attenuation at depth and a cleaner reflection at the ice–ocean boundary in radargrams.

There are processing techniques that can be used to glean additional information from the return signal of ice-penetrating radar (Figure 6). By using our camera to acquire stereo images, variations in surface topography can be included in the signal processing of the radargrams, which will reduce the level of surface scattering. In an incoherently processed radargram, the edges of fractures and cracks at interfaces will show as parabolas owing to the reflection at the corner, called corner reflectors. Using corner reflectors can assist in locating and measuring the width of fractures; see Figure 6(b). With additional processing, by accounting for Doppler shifts in return signal, higher-resolution radargrams can be produced. These 2D focused SAR processed radargrams will reveal any features within the ice shell that are within the bandwidth resolution and with a surface of $>30^{\circ}$; see Figure 6(c). In both the incoherently processed radargram and the 2D focused SAR processed radargram, any liquid water bodies within the shell will present strong reflections. In conjunction, the combination of surface topography, corner reflectors in the incoherent processed data, and inter-ice features at high inclination in 2D focused processed data present a rich data set that provide information on not only the ice shell thickness but also the inter-ice features and processes (see Figure 6).

6.5. Preservation of Organics

Enceladus flyby speeds must be managed such that each instrument can successfully collect the necessary data. The 20–50 km altitude constraint for the flyby is within the optimal range for sampling with MAW based on the expected densities of the plume vapor (Neveu et al. 2020), where lower altitudes correspond to higher plume vapor densities (Hansen et al. 2020). This altitude range is suitable for collecting between micron-sized particles from the collimated plume and nanometer-sized particles from the mixed plume vapor (MacKenzie et al. 2020). If the sample entering the mass spectrometer is faster than about $6\,\mathrm{km\,s^{-1}}$, critical information regarding organic structures may be destroyed through fragmentation (Postberg et al. 2018a; Klenner et al. 2020a; Jaramillo-Botero et al. 2021). However, our designed trajectory ensures that flyby velocities would not exceed $6\,\mathrm{km\,s^{-1}}$, and therefore we are unlikely to run into this issue.

6.6. Winter Is Coming

The 2039 January Enceladus equinox is a concern for missions that require visual images of the SPT of Enceladus. Starting in 2039 January, an increasing amount of the SPT, where the plume is located, will enter many-year periods of shadow (Figure 7). At the planned end of mission in 2040, regions south of 85° S will be in shadow until nearly 2055. This mission requires a relatively small number of visual images of the SPT that would all be captured in the first few flybys, and the flyby architecture enables flybys to occur relatively soon after Saturn orbit insertion, so this challenge would be less impactful for Tiger than it might be with alternative mission concept designs. Current information on NF5 (Niebur 2020) indicates that the estimated earliest launch readiness date is no earlier than fall 2031, more than a year later than the notional launch date for Tiger. If this constraint remains in the final NF5 AO, greater care must be taken to ensure that regions of interest for visual imaging will still be illuminated for nominal and contingency dates of science operation. Lack of surface illumination is not expected to be an issue for UV measurements of the plume that are back-lit from either solar or stellar sources. When attempting to image a surface region that is not sunlit 100% of the time, the spacecraft trajectory must be designed to arrive at a time when the surface area of interest is illuminated. As the daytime percentage falls, fewer favorable times are available, and the trajectory design problem becomes more constrained and difficult. The more constrained problem might be solvable with or without the use of additional fuel, or might sometimes be impossible to solve even for regions with nonzero daytime percentages depending on other problem variables (e.g., Saturn orbit insertion date, insertion orbit parameters, etc.). More detailed analysis with consideration for the exact spacecraft trajectory and surface regions of interest is required to determine the lower bound of acceptable daytime percentages. If visual imaging of shadowed regions is required, Saturn shine, light reflected from Saturn's disk, coupled with long exposures and better attitude control system performance could potentially be a solution.

6.7. Selecting a Power System

Designing an adequate power system was a significant challenge for this mission concept. Two Next-Gen RTGs were selected for the power system, given that MMRTGs and potential eMMRTGs did not have sufficient performance. Given that the solar irradiance at Saturn is a little less than 1/100 of that on Earth, solar arrays of a manageable size are not expected to be able to provide enough power (Spilker et al. 2009). MMRTGs and eMMRTGs could not be used for this study owing to their low power output at end of mission and high average annual power degradation. Next-Gen RTGs also have major advantages of significant mass and nuclear fuel savings while boosting the power by a factor of 1.5–2 over previous RTGs (Woerner 2017). Because the current TRL of Next-Gen RTGs ranges between 1 and 3, it is important to continue investing toward the development of high-performance thermoelectric materials and support maturation efforts for RTGs, so that the power requirements of future planetary science missions can be met.

6.8. Programmatic Risks

In order to inform the ocean worlds exploration community as it refines and evolves future mission concepts, we report several programmatic risks associated with the Tiger mission architecture. These risks include the following:

1. The MAW and ROAR instrument designs rely on the development of Europa Clipper's MASPEX and REASON analog instruments, respectively, which have yet to be demonstrated in flight as of this manuscript.
2. The spacecraft bus was intended to be provided by an industry contractor, and therefore specific alterations to the bus may be less flexible than one provided internally by NASA.
3. Any significant development of prelaunch challenges could jeopardize the Tiger mission by delaying the launch and pushing the Saturn orbit insertion timeline further into Enceladus's southern winter. Depending on the amount of delay, the quantity of science return may be

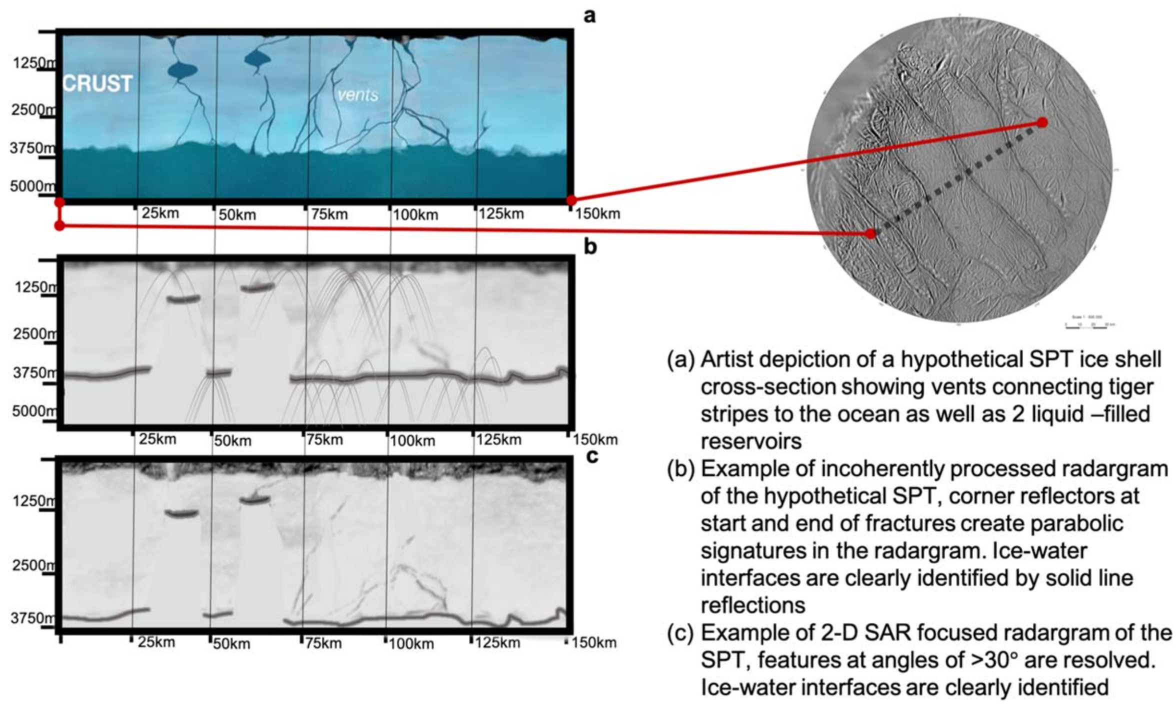

Figure 6. A theoretical cross section of the SPT with an artist's depiction of the underlying ice shell (a). Examples of both an incoherently processed radargram (b) and a 2D focused SAR radargram (c) modeled from the artist depiction are shown. SPT image (upper right) credit: Cassini Imaging Team, NASA. Artist depiction. (a) Upper left: credit to PSSS participant Alyssa Pascuzzo, modified from NASA/JPL: PIA23173.

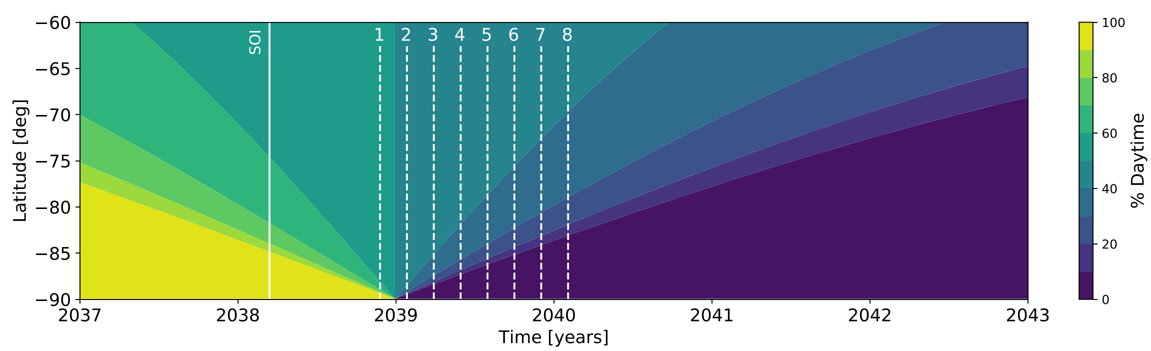

Figure 7. Surface illumination conditions in the southern hemisphere of Enceladus through time, with proposed Tiger flyby dates superimposed. For the mission timeline proposed in this study, Enceladus's south pole will begin to enter seasonal shadow before Tiger's second flyby.

proportionally reduced as the south pole becomes more shadowed, which is represented in Figure 7.

After analyzing the possible outcomes from the trades explained above, the mission architecture that showed the highest potential for high-quality science return within the NF cost, mass, and power limits was a habitability-focused mission with a flyby configuration. The instruments selected to achieve the mission objectives were optimized to fit the flyby configuration and budget limits and to deliver new scientific breakthroughs while leveraging space heritage of previous outer solar system missions.

7. Conclusion

The current research and understanding of ocean worlds were made possible through the information gathered by the Cassini–Huygens, Galileo, Voyager 1 and 2, and Pioneer 10 and 11 spacecraft. The Pioneer and Voyager programs gave the first glimpses of the surfaces of the outer planet satellites such as Enceladus, Europa, Titan, Ganymede, Callisto, and Triton. These images displayed the wide diversity of geology and surface compositions. Later measurements from Galileo and Cassini–Huygens provided higher-resolution imagery and more detailed measurements of the characteristics of these satellites, which pointed toward the likelihood that liquid water oceans were not unique to Earth within our solar system. There are now a multitude of confirmed and suspected ocean worlds within our solar system (Nimmo & Pappalardo 2016; Hand et al. 2020). The discoveries from these series of spacecraft over the past 50 yr have opened the prospect for comparative oceanography within our solar system.

One of the primary hurdles to rapid discoveries in the outer planets and their ocean satellites is the multidecade timescales required for the planning, development, launch, and flight time for these missions. This makes such missions costly relative to closer planetary targets such as the Moon or Mars. However, these ocean worlds have remained a predominant priority for NASA, proving the community's collective acknowledgment of the high potential for novel and extraordinary scientific return from ocean worlds. Specifically, liquid water is one of the primary drivers for life on Earth, so in the quest to understand origins of life and habitability on Earth, exploration of other liquid water reservoirs throughout the solar system is a rightfully compelling endeavor. In order to fully realize future science return, these highly compelling yet time-consuming ocean world mission targets demand careful future planning and sequenced, complementary investigations likely in conjunction with other space exploration agencies.

This is already being achieved through the current selection and development of the Europa Clipper (Phillips & Pappalardo 2014), Dragonfly (Turtle et al. 2017), and Jupiter Icy moons Explorer (JUICE; Lorente et al. 2017) missions, as well as the future planning of Europa Lander (Hand et al. 2018), Enceladus Orbilander (MacKenzie et al. 2020), Enceladus Life Finder (Reh et al. 2016), Explorer of Enceladus and Titan (Mitri et al. 2018), and Triton's Trident (Prockter et al. 2019). These missions aim to understand the potential for life at their target bodies and even the direct detection of life. The goals of these missions derive from the presence of liquid water and its connection to life on Earth. Realizing the potential for life and detection of life are not straightforward investigations (Neveu et al. 2018). Even on Earth, distinguishing signs of life from abiotic sources and directly detecting life can be difficult (Sagan et al. 1993). They require knowledge of the context in which measurements are taken, including, among others, instrument specifications, as well as environmental and situational conditions.

Tiger aims to close this knowledge gap between environmental conditions and interpretation of life detection results by providing habitability context to potential biomes within Enceladus, by isolating transport mechanisms for nutrients and energy. This will inform future life detection missions to Enceladus, and even other ocean worlds. As our knowledge and understanding of ocean worlds through comparative oceanography increases, so will the capability to understand and detect extinct or extant life elsewhere. As an NF mission concept, the provided funds are significantly less than what would be required for a lander, subsurface probe, or life detection mission. However, the knowledge gained from the Tiger mission concept will answer questions about Enceladus's nature that remove uncertainties and risks from future missions. The reduced risk and clearer picture of potential biomes, likely instrument requirements, and fewer operational uncertainties will pave the way for successful Flagship-class missions to both Enceladus and other ocean worlds.

The research was carried out at the Jet Propulsion Laboratory, California Institute of Technology, under a contract with the National Aeronautics and Space Administration (80NM0018D0004). This work was completed during session one of the 2020 NASA JPL PSSS. We acknowledge PSSS Administrator Joyce Armijo, JPL's Team X (Aron Wolf, David Sternberg, William Jones-Wilson, Jairus Hihn, William Smythe, Thaddaeus Voss, Roger Klemm, Eric Sunada, Melora Larson, Jeffrey Stuart, Ronald Hall, Daniel Kolenz, Gregory Welz, Mason Takidin, Jonathan Murphy, Matthew Kowalkowski, Elizabeth Luthman, and Christopher Landry), Damon Landau, and the specialists who evaluated the final presentation of this PSSS section (Amy Hofmann, Kim Reh, Morgan Cable, Curt Niebur, Paul Johnson, Randy Herrera). We also would like to thank Dr. Sarah Waller for her helpful input related to the mass spectrometry and Dr. Britney Schmidt for her guidance and feedback on the radar sections. We would like to thank NASA HQ Science Mission Directorate and the NASA Planetary Science Division for providing continued financial support for NASA JPL's PSSS. Pre-decisional information for planning and discussion purposes only.

ORCID iDs

Elizabeth M. Spiers https://orcid.org/0000-0003-0267-7472
Jessica M. Weber https://orcid.org/0000-0002-8434-0066
Chandrakanth Venigalla https://orcid.org/0000-0003-2776-568X
Andrew M. Annex https://orcid.org/0000-0002-0253-2313
Christine P. Chen https://orcid.org/0000-0001-7922-1743
Carina Lee https://orcid.org/0000-0001-8151-3438
Patrick Clifton Gray https://orcid.org/0000-0002-8997-5255
Kathleen J. McIntyre https://orcid.org/0000-0002-8307-144X
Jodi R. Berdis https://orcid.org/0000-0002-8572-0036
Shane R. Carberry Mogan https://orcid.org/0000-0002-0261-8117
Paula do Vale Pereira https://orcid.org/0000-0001-6162-9927
Saroj Kumar https://orcid.org/0000-0002-3843-3886
William O'Neill https://orcid.org/0000-0003-4790-5643
Elizabeth A. Czajka https://orcid.org/0000-0003-1874-4158
Perianne E. Johnson https://orcid.org/0000-0001-6255-8526
Sindhoora Tallapragada https://orcid.org/0000-0003-3190-1760
Jennifer Scully https://orcid.org/0000-0001-7139-8050

References

Barber, T. J. 2018, in American Institute of Aeronautics and Astronautics, Inc., 2018 Joint Propulsion Conf. (Reston, VA: AIAA), 4546
Barge, L. M., Flores, E., VanderVelde, D. G., et al. 2020, JGRE, 125, e06423
Blankenship, D. D., Young, D. A., Moore, W. B., & Moore, J. C. 2009, in Europa, ed. R. T. Pappalardo et al. (Tucson, AZ: Univ. Arizona Press), 631
Bouquet, A., Mousis, O., Waite, J. H., & Picaud, S. 2015, GeoRL, 42, 1334
Brockwell, T. G., Meech, K. J., Pickens, K., et al. 2016, in 2016 IEEE Aerospace Conf. (Piscataway, NJ: IEEE), 1, doi:10.1109/AERO.2016.7500777
Budney, C. J., Lowes, L. L., & Mitchell, K. L. 2018, LPSC, 46, 2736
Čadek, O., Tobie, G., VanÂ Hoolst, T., et al. 2016, GeoRL, 43, 5653
Carson, J. M., Johnson, A. E., Hines, G. D., et al. 2016, in GN&C Subsystem Concept for Safe Precision Landing of the Proposed Lunar MARE Robotic Science Mission (Reston, VA: AIAA), 1, doi:10.2514/6.2016-0100
Choblet, G., Tobie, G., Sotin, C., et al. 2017, NatAs, 1, 841
Cook, J. C., Stern, S. A., Feldman, P. D., et al. 2013, Icar, 225, 681
Dougherty, M. K., Buratti, B. J., Seidelmann, P. K., Spencer, J. R., & Dotson, R. 2018, in Enceladus and the Icy Moons of Saturn, ed. P. M. Schenk et al. (Tucson, AZ: Univ. Arizona Press), 3
Eigenbrode, J., Gold, R. E., McKay, C. P., Hurford, T., & Davila, A. 2018, in 42nd COSPAR Scientific Assembly 42 (Pasadena, CA), F3
Giese, B. & Cassini Imaging Team 2010, EPSC, 675
Gladstone, G. R., Persyn, S. C., Eterno, J. S., et al. 2017, SSRv, 213, 447
Gladstone, G. R., Stern, S. A., Retherford, K. D., et al. 2010, SSRv, 150, 161
Glein, C. R., Baross, J. A., & Waite, J. H. 2015, GeCoA, 162, 202
Goldstein, D. B., Hedman, M., Manga, M., et al. 2018, in Enceladus and the Icy Moons of Saturn, ed. P. M. Schenk et al. (Tuscon, AZ: Univ. Arizona Press), 175
Gordon, S., & Kern, D. 2015, in 29th Aerospace Testing Seminar (Pasadena, CA: JPL, Caltech), https://ntrs.nasa.gov/citations/20150020490
Guzman, M., Lorenz, R., Hurley, D., et al. 2019, IJAsB, 18, 47

Hand, K. P., Phillips, C. B., Hofmann, A., et al. 2018, AGUFM, 2018, P52C-03
Hand, K. P., Sotin, C., Hayes, A., & Coustenis, A. 2020, SSRv, 216, 95
Hansen, C. J., Esposito, L., Colwell, J., et al. 2020, Icar, 344, 113461
Hansen, C. J., Esposito, L., Stewart, A. I. F., et al. 2006, Sci, 311, 1422
Hendrix, A. R., Hurford, T. A., Barge, L. M., et al. 2019, AsBio, 19, 1
Hendrix, A. R., Noll, K. S., & Spencer, J. R. 2015, AGUFM, 2015, P31B-2072
Howell, S. M., & Pappalardo, R. T. 2020, NatCo, 11, 1311
Hsu, H.-W., Postberg, F., Sekine, Y., et al. 2015, Natur, 519, 207
Iess, L., Stevenson, D. J., Parisi, M., et al. 2014, Sci, 344, 78
Imken, T., Castillo-Rogez, J., He, Y., Baker, J., & Marinan, A. 2017, in 2017 IEEE Aerospace Conf. (Piscataway, NJ: IEEE), 1, doi:10.1109/AERO.2017.7943885
Jaramillo-Botero, A., Cable, M. L., Hofmann, A. E., et al. 2021, AsBio, 21, 421
Jaumann, R., Stephan, K., Hansen, G. B., et al. 2007, EPSC, 2007, 636
Kempf, S., Horányi, M., Hsu, H.-W., et al. 2018, in Enceladus and the Icy Moons of Saturn, ed. P. M. Schenk et al. (Tucson, AZ: Univ. Arizona Press), 195
Khawaja, N., Postberg, F., Hillier, J., et al. 2019, MNRAS, 489, 5231
Kite, E. S., & Rubin, A. M. 2016, PNAS, 113, 3972
Klenner, F., Postberg, F., Hillier, J., et al. 2020a, AsBio, 20, 179
Klenner, F., Postberg, F., Hillier, J., et al. 2020b, AsBio, 20, 1168
Leitner, J. 2014, Risk Classification and Risk-based Safety and Mission Assurance, https://ntrs.nasa.gov/api/citations/20150001352/downloads/20150001352.pdf
Lorente, R., Altobelli, N., Vallat, C., et al. 2017, in 19th EGU General Assembly Conf. Proc. (Vienna), 14611
Lowes, L., Mitchell, K., Scully, J., et al. 2020, AAS/DPS Meeting, 52, 502.11
Lucchetti, A., Pozzobon, R., Mazzarini, F., Cremonese, G., & Massironi, M. 2016, AAS/DPS, 48, 214.01
MacKenzie, S. M., Neveu, M., Davila, A., et al. 2020, LPICo, 2547, 6034
Magee, B. A., & Waite, J. H. 2017, LPSC, 28, 2974
Matthes, C. S. R., Woerner, D. F., Hendricks, T. J., et al. 2018, in 2018 IEEE Aerospace Conf. (Piscataway, NJ: IEEE), 1, doi:10.1109/AERO.2018.8396738
McKay, C., Davila, A., Eigenbrode, J., et al. 2020, Contamination Control Technology Study for Achieving the Science Objectives of Life-Detection Missions, TM-20205008709, https://science.gsfc.nasa.gov/sed/content/uploadFiles
McKay, C. P., Davila, A., Glein, C. R., et al. 2018, in Enceladus and the Icy Moons of Saturn, ed. P. M. Schenk et al. (Tucson, AZ: Univ. Arizona Press), 437
Ménez, B., Pisapia, C., Andreani, M., et al. 2018, Natur, 564, 59
Mitri, G., Postberg, F., Soderblom, J. M., et al. 2018, P&SS, 155, 73
Mrozinski, J. 2018, in NASA Instrument Cost Model: Version VIII: NICM VIII Training Workshop (Pasadena, CA: Jet Propulsion Laboratory, National Aeronautics and Space)
NASA 2004, NASA Procedural Requirements 8 705.4-2004, https://nodis3.gsfc.nasa.gov/npg_img/N_PR_8705_0004_/N_PR_8705_0004_.pdf
National Academies of Sciences, Engineering, and Medicine 2018, Visions into Voyages for Planetary Science in the Decade 2013-2022: A Midterm Review (Washington, DC: The National Academies Press)
Neveu, M., Anbar, A., Davila, A. F., et al. 2020, FrASS, 7, 26
Neveu, M., Hays, L. E., Voytek, M. A., New, M. H., & Schulte, M. D. 2018, AsBio, 18, 1375
Niebur, C. 2016, Announcement of Opportunity New Frontiers 4, https://newfrontiers.larc.nasa.gov/NF4/announcements.html
Niebur, C. 2020, Second Community Announcement: Advance Notice Regarding NF5 AO, https://newfrontiers.larc.nasa.gov/NF5/pdf_files/NF5%20Second%20Community%20Announcement.pdf
Nimmo, F. 2020, PNAS, 117, 16107
Nimmo, F., & Pappalardo, R. T. 2016, JGRE, 121, 1378
Nimmo, F., Spencer, J. R., Pappalardo, R. T., & Mullen, M. E. 2007, Natur, 447, 289
Phillips, C. B., & Pappalardo, R. T. 2014, EOSTr, 95, 165
Porco, C., DiNino, D., & Nimmo, F. 2014, AJ, 148, 45
Porco, C. C., Helfenstein, P., Thomas, P. C., et al. 2006, Sci, 311, 1393
Postberg, F., Clark, R. N., Hansen, C. J., et al. 2018a, in Enceladus and the Icy Moons of Saturn, ed. P. M. Schenk et al. (Tucson, AZ: Univ. Arizona Press), 129
Postberg, F., Kempf, S., Hillier, J., et al. 2008, Icar, 193, 438
Postberg, F., Kempf, S., Schmidt, J., et al. 2009, Natur, 459, 1098
Postberg, F., Khawaja, N., Abel, B., et al. 2018b, Natur, 558, 564
Postberg, F., Schmidt, J., Hillier, J., Kempf, S., & Srama, R. 2011, Natur, 474, 620
Prockter, L. M., Mitchell, K. L., Howett, C. J. A., et al. 2019, LPSC, 50, 3188
Ramanathan, R., & Korfmacher, W. 2016, Bioanalysis, 8, 1639
Rathbun, J. A., & Spencer, J. R. 2020, Icar, 338, 113500
Reh, K., Spilker, L., Lunine, J. I., et al. 2016, in IEEE Aerospace Conf. (Piscataway, NJ: IEEE), 1, doi:10.1109/AERO.2016.7500813
Sagan, C., Thompson, W. R., Carlson, R., Gurnett, D., & Hord, C. 1993, Natur, 365, 715
Schmidt, B., Craft, K., Cwik, T., et al. 2021, BAAS, 53, 246
Schmidt, J., Brilliantov, N., Spahn, F., & Kempf, S. 2008, Natur, 451, 685
Sierks, H., Keller, H. U., Jaumann, R., et al. 2011, SSRv, 163, 263
Spahn, F., Schmidt, J., Albers, N., et al. 2006, Sci, 311, 1416
Spencer, J. 2010a, Planetary Science Decadal Survey Enceladus Orbiter, Mission Concept Study (Washington, DC: NASA), https://sites.nationalacademies.org/cs/groups/ssbsite/documents/webpage/ssb_059320.pdf
Spencer, J. 2010b, Planetary Science Decadal Survey JPL Rapid Mission Architecture (RMA) Enceladus Study Final Report (Washington, DC: NASA), http://ia800500.us.archive.org/3/items/EnceladusFlybySampleReturnConceptStudies/21_Enceladus-Flyby-Sample-Return-Final.pdf
Spencer, J. R., Nimmo, F., Ingersoll, A. P., et al. 2018, in Enceladus and the Icy Moons of Saturn, ed. P. M. Schenk et al. (Tucson, AZ: Univ. Arizona Press), 163
Spilker, T. R., Moeller, R. C., Borden, C. S., et al. 2009, in 2009 IEEE Aerospace Conf. (Piscataway, NJ: IEEE), 1, doi:10.1109/AERO.2009.4839317
Spitale, J. N., Hurford, T. A., Rhoden, A. R., Berkson, E. E., & Platts, S. S. 2015, Natur, 521, 57
Srama, R., Ahrens, T. J., Altobelli, N., et al. 2004, SSRv, 114, 465
Stern, S. A., Slater, D. C., Scherrer, J., et al. 2008, SSRv, 140, 155
Thomas, P. C., Tajeddine, R., Tiscareno, M. S., et al. 2016, Icar, 264, 37
Turtle, E. P., Barnes, J. W., Trainer, M. G., et al. 2017, LPSC, 48, 1958
Waite, J. H., Combi, M. R., Ip, W.-H., et al. 2006, Sci, 311, 1419
Waite, J. H., Glein, C. R., Perryman, R. S., et al. 2017, Sci, 356, 155
Waite, J. H., Lewis, W. S., Kasprzak, W. T., et al. 2004, SSRv, 114, 113
Waite, J. H., J., Lewis, W. S., Magee, B. A., et al. 2009, Natur, 460, 487
West, R., Gim, Y., Tan, I., & Hawkins, D. 2017, Radar Ambiguities and Signal Processing Design Tradeoffs in the REASON Radar Sounder (Pasadena, CA: JPL, NASA), http://hdl.handle.net/2014/47480
Wie, B., Lappas, V., & Gil-Fernández, J. 2014, The International Handbook of Space Technology (Berlin: Springer), 323
Woerner, D. 2017, in Next-Generation RTGs for NASA (Pasadena, CA: JPL, NASA), http://hdl.handle.net/2014/46421
Woerner, D. F. 2018, in Plans and Concepts for a New Generation of RTGs for Planetary Science Missions (Pasadena, CA: JPL, NASA), https://trs.jpl.nasa.gov/handle/2014/48692
Zolotov, M. Y. 2007, GeoRL, 34, L23203